DIGITAL ACCESS TO SCHOLARSHIP AT HARVARD

Nano-sized SQUID-on-tip for scanning probe microscopy

(Article begins on next page)

Nano-sized SQUID-on-tip for scanning probe microscopy

A Finkler[1], D Vasyukov[1], Y Segev[1], L Neeman[1], Y Anahory[1], Y Myasoedov[1], M L Rappaport[1], M E Huber[2], J Martin[3], A Yacoby[4] and E Zeldov[1]

[1]Department of Condensed Matter Physics, Weizmann Institute of Science, Rehovot 76100, Israel

[2]Departments of Physics and Electrical Engineering, University of Colorado, Denver, CO 80217, USA

[3]School of Physics, University of Exeter, Stocker Road, Exeter, EX4 4QL, United Kingdom

[4]Department of Physics, Harvard University, MA 02138, USA

E-mail: `amit.finkler@weizmann.ac.il`, `denis.vasyukov@weizmann.ac.il`

Abstract. We present a SQUID of novel design, which is fabricated on the tip of a pulled quartz tube in a simple 3-step evaporation process without need for any additional processing, patterning, or lithography. The resulting devices have SQUID loops with typical diameters in the range 75 - 300 nm. They operate in magnetic fields up to 0.6 T and have flux sensitivity of 1.8 $\mu\Phi_0/\mathrm{Hz}^{1/2}$ and magnetic field sensitivity of 10^{-7} $\mathrm{T/Hz}^{1/2}$, which corresponds to a spin sensitivity of 65 $\mu_\mathrm{B}/\mathrm{Hz}^{1/2}$ for aluminum SQUIDs. The shape of the tip and the small area of the SQUID loop, together with its high sensitivity, make our device an excellent tool for scanning SQUID microscopy: With the SQUID-on-tip glued to a tine of a quartz tuning fork, we have succeeded in obtaining magnetic images of a patterned niobium film and of vortices in a superconducting film in a magnetic field.

1. Introduction

For more than a decade, modern magnetic imaging techniques have been used for studying small magnetic moments: single molecular magnets [1,2], magnetic nanoparticles [3,4], spin ice systems [5,6], and, the ultimate limit, the detection of a single spin [7]. The detection tools for these objects are diverse and range from magnetic resonance force microscopy [7] and spectroscopy of nitrogen-vacancy centers in diamond [8] to superconducting quantum interference devices (SQUIDs) [9-11]. The latter offer the least invasive and the most direct measurement of magnetic fields. However, conventional lithographically-produced SQUIDs are not well suited for measuring small magnetic moments since the coupling between the SQUID loop and the magnetic object, and thus its spin sensitivity, directly depend on the size of the loop and its distance from the object [10,11]. For this reason, nano-SQUID research has become popular of late. The vast majority of nano-SQUIDs that have been produced and studied have had planar geometry [9,12-17], and a great deal of effort has been made to to minimize the distance between the SQUID loop and the specimen, e.g., by placing the specimen in direct contact with the SQUID loop [9]. When scanning is desired, great lengths are taken to position the SQUID very close to the edge of the substrate but, nevertheless, it has proven to be extremely difficult
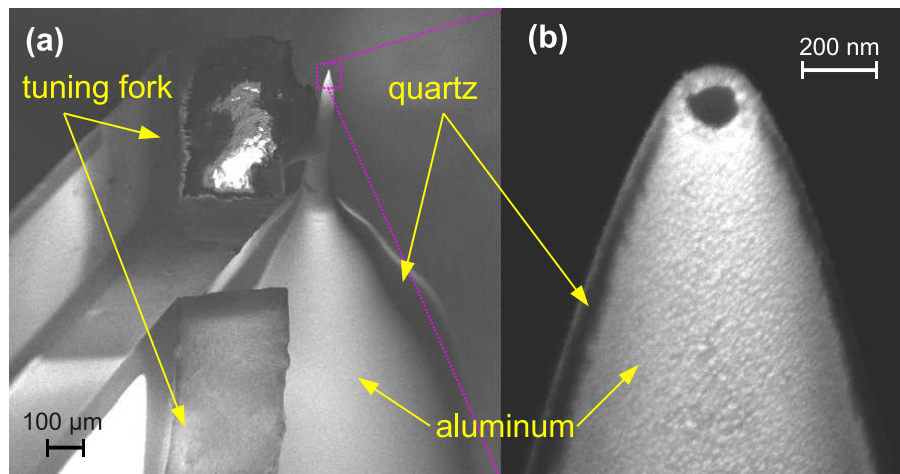
Figure 1. (a) SEM image of the nano-SQUID glued to one tine of a quartz tuning fork (the bottom part of the tip is distorted due to the large SEM field of view). (b) Magnification of tip in (a). Aluminum is evaporated onto opposite sides of the tube, forming two superconducting leads (bright) separated by a bare quartz gap (dark), and onto the apex ring that forms the nano-SQUID loop. The parts of the loop that are in contact with the leads form strong superconducting regions while the segments between the leads form weak links acting as the two Josephson junctions of the SQUID.

with planar SQUIDs to achieve the proximity to the object necessary to image a single spin. The most sensitive planar scanning SQUID to date can get as close as 0.3 μm to the sample surface and has a sensitivity of 70 $\mu_B/\text{Hz}^{1/2}$ at 4 K [12]. In our research we concentrated on producing a nano-SQUID loop on the apex of a tip and have coupled it to a quartz tuning fork [18]. This combination enables scanning within a distance of a few nanometers with very high spin sensitivity. Here we present the design and characteristics of a SQUID-on-tip (SoT) together with magnetic images measured on a test sample.

2. SQUID-on-tip fabrication

The fabrication process consists of the following steps: first, a 1 mm dia. fused quartz tube is heated to a temperature close to its melting point using a commercial micropipette puller [19] and pulled until it breaks, giving two sharp tips of the same size. The resulting size of the tips depends on the pulling parameters and can be varied between 20 and 2000 nm. Next, thick indium leads are soldered onto the surface of the non-pulled part of the tip, i.e., where the original tube diameter is preserved. The third stage is a three-step evaporation process in which a superconducting material (in this case 25 nm thick aluminum) is thermally evaporated first onto both sides of the tip, and then 17 nm of aluminum are evaporated onto the apex of the tip. The resulting scanning electron microscope (SEM) images are shown in Fig. 1. The superconductors on the sides of the tip form superconducting leads with strong superconductivity, whereas the material on the ring creates weak links of the Dayem bridge type. The resulting nano-SQUID requires no lithographic processing whatsoever and is ready to use. Its position on the apex of a quartz tube is ideal for scanning SQUID microscopy measurements [18].

3. Characteristics of the SQUID-on-tip

The fabricated SoTs were characterized in a ^{3}He cryostat at a temperature of 0.3 K, which is well below their superconducting transition ($T_c \approx 1.6$ K). The SoTs were shunted by a parallel 2 Ω

resistor located approximately 20 cm from the SoT and connected to it using superconducting niobium-titanium wires and biased in a with a current source (The normal state resistance of the SQUID was 90 Ω). The SQUID therefore operated in a quasi-constant-voltage mode, thereby minimizing hysteresis and providing stable DC-biased SQUID operation. The SoT was connected in series with the input coil of a SQUID series-array amplifier (SSAA) [20], working in a flux-locked loop (FLL) mode [21], its current (I_{SoT}) was measured by measuring the voltage drop on a 5 kΩ feedback resistor. The resulting I-V characteristics of our SoTs exhibit stable, non-
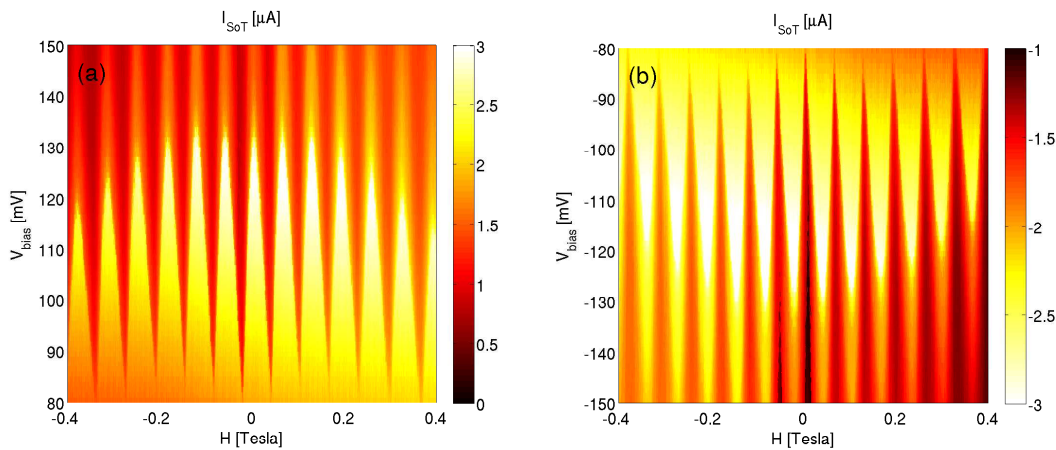

Figure 2. Quantum interference patterns of the SoT current $I_{\text{SoT}}(V_{\text{in}}, H)$ at 300 mK at positive (a) and negative (b) voltage bias. The patterns are asymmetric both in field and in bias and are almost out of phase for the two bias polarities.

hysteretic behavior with a wide negative-resistance region above the critical current (I_c). This effect is consistent with the Aslamazov-Larkin model of a single Josephson junction connected in our bias configuration [22]. Unlike most small SQUIDs, which demonstrate significant reduction of modulation of their I_c with magnetic field compared to larger SQUIDs of the same design [17], the SoTs show deep modulation of $I_c(H)$. This has already been discussed in detail elsewhere [18]. Figure 2 shows a pronounced $I_{\text{SoT}}(V_{\text{in}}, H)$ quantum interference pattern with a period of 60.8 mT, which corresponds to an effective SQUID diameter of 208 nm. The critical current modulation $I_c^{\text{max}}/I_c^{\text{min}} = 1.67$ is large. It must be noted that the SoT demonstrates a strong asymmetry between positive and negative biases and the interference patterns for these biases are almost out of phase. This asymmetry arises from the difference in critical currents of the two junctions forming the SQUID and is in fact beneficial for the device operation, since the high sensitivity linear region of $I_c(H)$ can be found over a wider range of fields by choosing an appropriate bias polarity. Our theoretical fit of $I_c(H)$ [23] yielded the following parameters: the critical currents of the two junctions $(1 - \alpha)I_0 = 0.8$ µA and $(1 + \alpha)I_0 = 2.4$ µA, where $I_0 = 1.6$ µA, the asymmetry parameter $\alpha = 0.5$, and $\beta = 2LI_0/\Phi_0 = 0.85$, where L is the loop inductance and $\Phi_0 = h/2e$ is the flux quantum.

β equal to 0.85 for the SoT implies a large inductance: $L = 549$ pH. If this value is compared to the geometrical inductance of the SQUID loop $L_g = \mu_0 R(\log(8R/r)) = 0.26$ pH, where $R = 104$ nm is the loop radius and $r = 15$ nm is the radius of the loop wire, it becomes obvious that our device, due to its small size, is mostly governed by the kinetic inductance [24] of the loop, $L_k = 2\pi\mu_0\lambda_L^2 R/a$, where $a = t \times w = 510$ nm^2 is the estimated cross-section of the loop wire (the film thickness, t, is 17 nm and the loop width, w, is approximately 30 nm) and $\lambda_L = 0.58$ µm is the resulting penetration depth of the aluminum film. This value is larger than that of the bulk material, but still plausible for thin films [25]. Unlike conventional SQUIDs,

which normally operate only at rather small fields, our SoTs show substantial oscillations even at fields as high as 0.4 T (Fig. 2). This provides yet another unique advantage of our devices. This tolerance to relatively high magnetic fields apparently arises from the tip geometry, where all the parts of the SQUID, except its weak links are along the quartz tube and, thus, are almost parallel to the external magnetic field. The films are also very thin.

The flux sensitivity of a SQUID is limited by its intrinsic noise, which we have already reported in details elsewhere [18]. In our SoTs, the flux noise changes from $1/f$ for frequencies up to a few tens of Hz to white noise at the level of 1.8×10^{-6} $\Phi_0/\mathrm{Hz}^{1/2}$. This flux sensitivity is comparable with that of currently available larger SQUIDs [26]. However, the loop area of our devices is only 0.034 μm^2, which is the smallest reported to date [18] and makes it ideal for studying small magnetic moments, since the spin sensitivity in units of $\mu_\mathrm{B}/\mathrm{Hz}^{1/2}$ is given by:

$$S_n = \Phi_n \frac{R}{r_e} \left(1 + \frac{h^2}{R^2} \right)^{3/2} \tag{1}$$

where R is the radius of the loop, h is the height of the loop above the magnetic dipole, $r_e = 2.82 \times 10^{-15}$ m is the electron radius, and Φ_n is the flux noise in units of $\Phi_0/\mathrm{Hz}^{1/2}$ [19]. If $h < R$, then for spins situated in the center of loop and oriented normal to the loop plane we obtain a spin sensitivity $S_n \approx 65$ $\mu_\mathrm{B}/\mathrm{Hz}^{1/2}$. This value, however, can be enhanced by placing the magnetic moments not in the center of the loop, but near the edge of the loop [10,11]. In this case, R in Eq. 1 is replaced by r (15 nm versus 104 nm), leading to a predicted sensitivity of 33 $\mu_\mathrm{B}/\mathrm{Hz}^{1/2}$. This sensitivity should be enough to image a single molecular magnet, e.g., Mn$_{12}$-acetate with a moment of 20 $\mu_\mathrm{B}/\mathrm{Hz}^{1/2}$ [27], by integrating the signal over a few seconds. Assuming that the flux noise would not increase drastically, further reduction of the SoT size, (we are able to produce working SQUIDs with diameters of 75 nm), could help us reach a sensitivity below 20 $\mu_\mathrm{B}/\mathrm{Hz}^{1/2}$.

4. Microscope design

The design of the scanning part of our measurement setup was largely inspired by near-field scanning optical microscopes (NSOMs) that utilize optical fibers and a quartz tuning fork (TF) to detect the approach of the tip to the sample's surface [28]. The SoT tip was glued to one tine of a TF and the frequency shift of the TF resonance peak was used as a measure of the proximity to the sample's surface. This technique allows simultaneous measurements of the sample's topography and the local magnetic fields. The test sample was positioned on a commercial [29] X-Y-Z piezo-scanner driven by an SPM controller and a PLL [30, 31].

5. Measurements: Nb serpentine

As a test sample we used a 200 nm thick niobium film, deposited using an e-gun while keeping the substrate at a temperature of 200 °C in a background pressure of 10^{-6} Torr and patterned as a serpentine. With such a geometry, one can drive a current through the entire sample and measure its corresponding self-field while also being able to obtain the magnetic signal resulting from the Meissner effect and, when close enough to the sample, observe vortices. We applied an AC current of 3 mA at a frequency of 13.44 kHz and measured the resulting self-field using the SoT concurrently with the topography measured from the tuning fork's frequency shift. These two measurements are shown in Fig. 3. The self-field image agrees with the theoretical (Biot-Savart law) calculation of the magnetic field emanating from a current through a superconducting thin strip and closely follows the topography.

Figure 4 shows the DC magnetic signal a few nm above the double-edged funnel-shaped region in the serpentine shown in Fig. 3. The sample was field-cooled at an applied magnetic field of 20 Gauss. The vortex lattice is highly disordered, due to the strong pinning in the Nb film at such
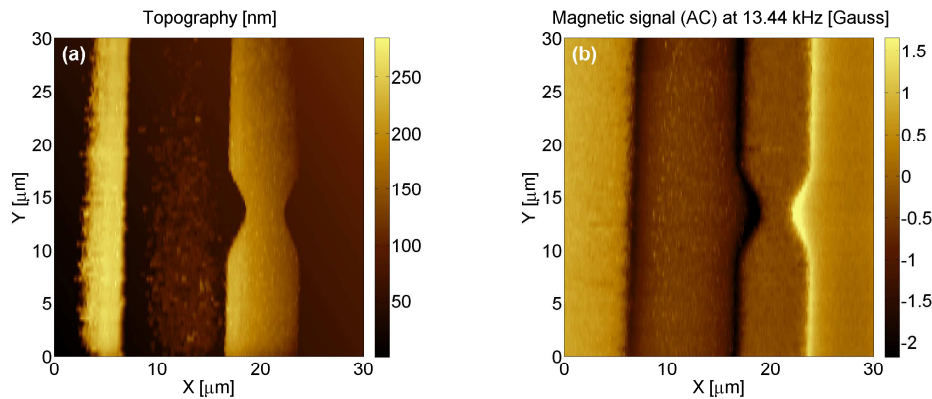
Figure 3. (a) A topographic measurement of the Nb serpentine showing a double-edged funnel in the central part of the strip; (b) A self-field measurement of the same serpentine with a current of 3 mA at 13.44 kHz.

a low temperature. Figure 4(c) shows a topographic measurement of the same region, taken in our setup, showing the granular structure of the Nb film.
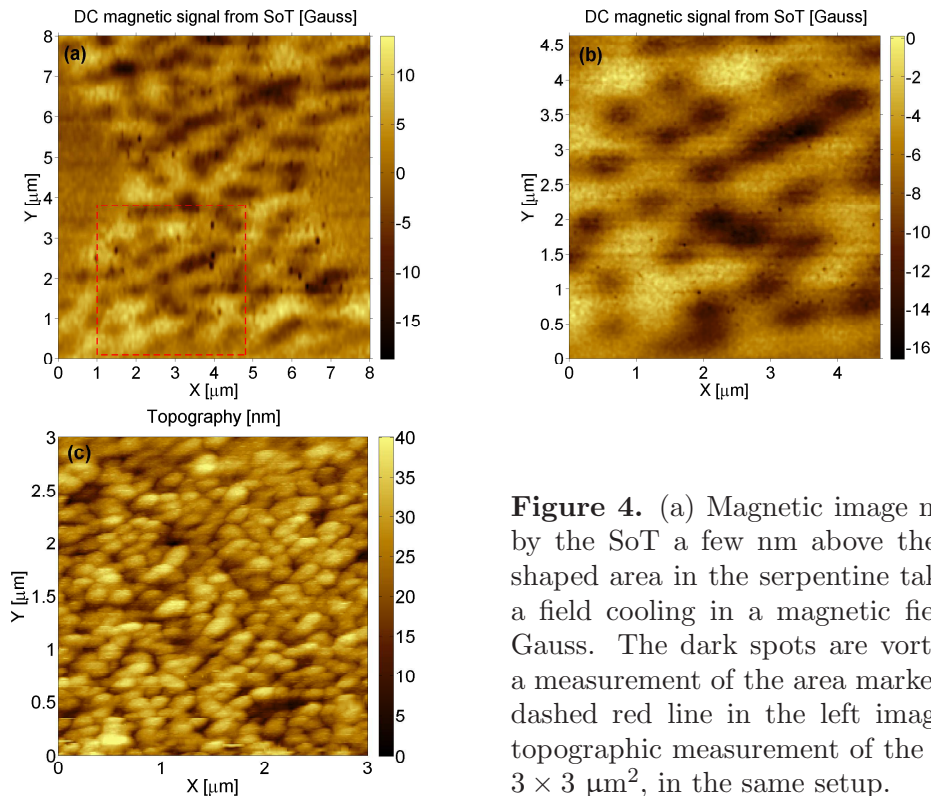

Figure 4. (a) Magnetic image measured by the SoT a few nm above the funnel-shaped area in the serpentine taken after a field cooling in a magnetic field of 20 Gauss. The dark spots are vortices; (b) a measurement of the area marked by the dashed red line in the left image; (c) a topographic measurement of the Nb film, 3×3 μm^2, in the same setup.

6. Conclusion

We have demonstrated a novel SQUID-on-tip device, which allows positioning of a SQUID a few nanometers from an object of study. The resulting devices have the smallest loop area reported so far of 0.034 μm^2, operate at fields as high as 0.6 T, and have flux sensitivity of 1.8×10^{-6} Φ_0/Hz$^{1/2}$, which translates to a spin sensitivity of 65 μ$_B$/Hz$^{1/2}$. We also demonstrated

the application of one of our devices as magnetic sensor in a scanning SQUID microscope and obtained images of the magnetic field pattern of a test sample, including images of vortex matter in a superconducting niobium film. With a further reduction of the SoT loop size and the enhancement of the SQUID sensitivity by sensing the magnetic moments situated near the SQUID ring, we expect a further substantial increase of the SoT performance.

Acknowledgments

References

[1] Sessoli R, Gatteschi D, Caneschi A and Novak M A 1993 *Nature (London)* **365** 141
[2] Sangregorio C, Ohm T, Paulsen C, Sessoli R and Gatteschi D 1997 *Phys. Rev. Lett.* **78** 4645
[3] Skumryev V, Stoyanov S, Zhang Y, Hadjipanayis G, Givord D and Nogués J 2003 *Nature* **423** 850
[4] Sun S, Murray S B, Weller D, Folks L and Moser A 2000 *Science* **287** 1989
[5] Bramwell S T and Gingras M J P 2001 *Science* **294** 1495
[6] Castelnovo C, Moessner R and Sondhi S L 2007 *Nature* **451** 42
[7] Rugar D, Budakian R, Mamin H J and Chui B W 2004 *Nature* **430** 329
[8] Maze J R, Stanwix P L, Hodges J S, Hong S, Taylor J M, Cappellaro P, Jiang L, Dutt M V G, Togan E, Zibrov A S, Yacoby A, Walsworth R L and Lukin M D 2008 *Nature* **455** 644
[9] Cleuziou J-P, Wernsdorfer W, Bouchiat V, Ondarçuhu T and Monthioux M 2006 *Nature Nanotech.* **1** 53
[10] Bouchiat V 2009 *Supercond. Sci. Technol.* **22** 064002
[11] Tilbrook D L 2009 *Supercond. Sci. Technol.* **22** 064003
[12] Koshnick N C, Huber M E, Bert J A, Hicks C W, Large J, Edwards H and Moler K A 2008 *Appl. Phys. Lett.* **93** 243101
[13] Hasselbach K, Ladam C, Dolocan V O, Hykel D, Crozes T, Schuster K and Mailly D 2008 *J. Phys. Conf. Series* **97** 012330
[14] Hao L, Mann C A, Gallop J C, Cox D, Ruede F, Kazakova O, Josephs-Franks P, Drung D and Schurig T 2011 *Appl. Phys. Lett.* **98** 092504
[15] Granata C, Vettoliere A, Russo R, Esposito E, Russo M and Ruggiero B 2009 *Appl. Phys. Lett.* **94** 062503
[16] Romans E J, Osley E J, Young L, Warburton P A and Li W 2010 *Appl. Phys. Lett.* **97** 222506
[17] Troeman A G P, Derking H, Borger B, Pleikies J, Veldhuis D and Hilgenkamp H 2007 *Nano Lett.* **7** 2152
[18] Finkler A, Segev Y, Myasoedov Y, Rappaport M L, Neeman L, Vasyukov D, Zeldov E, Huber M E, Martin J and Yacoby A 2010 *Nano Lett.* **10** 1046
[19] Sutter Instruments P-2000
[20] Huber M E, Neil P A, Benson R G, Burns D A, Corey A F, Flynn C S, Kitaygorodskaya Y, Massihzadeh O, Martinis J M and Hilton G C 2001 *IEEE Trans. Appl. Supercond.* **11** 4048
[21] Seton H C, Hutchison J M S and Bussell D M 1997 *IEEE Trans. Appl. Supercond.* **7** 3213
[22] Aslamazov L G and Larkin A I 1969 *JETP Lett.* **9** 87
[23] Tesche C D and Clarke J 1977 *J. Low Temp. Phys.* **29** 301
[24] Penin N A, Golovashkin A I and Guro G M 1996 *Phys. Solid State* **38** 823
[25] Gershenson M and McLean W L 1982 *J. Low Temp. Phys.* **47** 123
[26] Kleiner R, Koelle D, Ludwig F and Clarke J 2004 *Proc. IEEE* **92** 1534
[27] Lam S K H, Yang W, Wiogo H T R, Foley C P 2008 *Nanotechnology* **19** 285303
[28] Karrai K and Grober R D 1995 *Appl. Phys. Lett.* **66** 1842
[29] atto**cube** systems ANSxyz100
[30] RHK Technology SPM 1000 R8.5
[31] atto**cube** systems ASC500